Korean J. Chem. Eng., 33(4), 1181-1185 (2016)
DOI: 10.1007/s11814-015-0264-y

pISSN: 0256-1115
eISSN: 1975-7220

Development and performance analysis of a novel agitated vessel

Gomadurai Chinnasamy*,†, Saravanan Kaliannan*, Abraham Eldho, and Deepa Nadarajan*****

*Department of Chemical Engineering, Kongu Engineering College, Perundurai, Erode-638052, Tamilnadu, India
**Department of Chemical Engineering, Dire Dawa Institute of Technology, Dire Dawa University, Dire Dawa, Ethiopia
***Department of Chemical Engineering, St. Joseph's College of Engineering,
Semmencherry, Chennai-600119, Tamilnadu, India
(*Received 9 September 2015 • accepted 26 November 2015*)

Abstract−The objective of the present study was to design, fabricate and evaluate the performance of a novel air-inducing impeller system with a specially designed air-inducing tube-set. The novel air-inducing impeller system, when attached to a conventional baffled agitated vessel, could convert it into an air-inducing reactor. Water was used as the working fluid and the characteristics of the impeller system such as critical speed, power consumption and gas holdup were investigated by varying the gas free liquid level, orifice immersion depth, bottom clearance and impeller speed. Results showed that this novel air-inducing impeller system induced the air at speeds lower than the critical speeds reported by most of the investigators in the literature.

Keywords: Air-inducing Impeller, Self-ingesting Reactor, Critical Speed, Gas Holdup, Hydrodynamics

INTRODUCTION

Mixing of gas and liquid in a stirred tank is a widely known industrial process. Conventional gas-liquid reactors are equipped with sparger at the bottom of the vessel to disperse the gas into the liquid [1]. When the conversion of gas per pass is very low or when pure gases are used, recirculation of gas from the head space back into the liquid is required in a gas-liquid reaction system [2-7]. Gas-inducing reactor is used to disperse the unreacted overhead gas phase into the liquid in an agitated reactor without gas outlet. In a gas-inducing impeller, the pressure difference between the head-space and the local pressure at the orifice in the impeller is the driving force for gas induction [6]. The self-inducing impellers found in literature are of two types: (1) hollow shaft with hollow blade type, and (2) stator and rotor type [6,8,9]. A gas-inducing reactor induces the gas available above the head space to flow into the liquid when the impeller speed exceeds the critical rotational speed (N_C) of the impeller [10]. At impeller speeds lower than the critical speed, no aeration of the liquid takes place [5]. Hydrogenation, ammonolysis, alkylation, ozonolysis, hydrochlorination, oxidation, suspension polymerization, oxidative leaching of ores, wastewater treatment are some of the typical applications of gas inducing reactors [6,9,11-16].

The literature analysis showed that most researchers have developed air-inducing impeller systems consisting of hollow impeller and hollow shaft, which have a common limitation that the impellers reported in the literature cannot readily convert a conventional agitated vessel into air-inducing reactor. Hence, the present study endeavors to demonstrate a novel method for the air-inducing mechanism. A conventional agitated vessel was converted into an air-inducing reactor by attaching a specially designed air-inducing tube set to the impeller shaft. The performance characteristics of the present system such as critical speed, power consumption and gas holdup were investigated by varying the gas free liquid level, orifice immersion depth, bottom clearance and impeller speed taking water as the working fluid.

EXPERIMENTAL

A flat-bottomed cylindrical agitated vessel (0.455 m ID, 0.012 m wall thickness, and 0.57 m height), made of acrylic material, was mounted on a torque-table fixed to the floor. Four vertical baffles were fitted to seize the vortex formation and ensure effective mixing of the working fluid. The impeller diameter and the baffle width were 1/3 and 1/10 of the inner diameter of tank, respectively. The impeller, mounted on a vertical solid shaft, was driven by a 2 hp, 3 phase AC induction motor (Monark, India). The air-inducing tube set used for inducing air into the vessel was fabricated by using six stainless steel tubes (SS316, 0.01 m OD, 0.007 m ID) bent to 'L' shape and welded vertically to two hub rings (0.01 m ID, 0.025 m OD) at equiangular radial array with the horizontal ends facing outwards (Fig. 1).

The tube-ends at the horizontal section of the tube bundle were closed and those of the vertical section were left open. There were eight 0.002 m orifices arranged in two opposite rows in the horizontal section of each tube in the tube bundle. The air-inducing tube set was attached to the impeller shaft by scrub screws to make the tube bundle run along with the impeller shaft. The diameter of the air-inducing tube set is equal to that of the impeller. For all experimental runs, the horizontal section of the tube bundle was immersed in the liquid and the tube ends at the vertical section were above the liquid level in the reactor.

†To whom correspondence should be addressed.
E-mail: cgomadurai@gmail.com

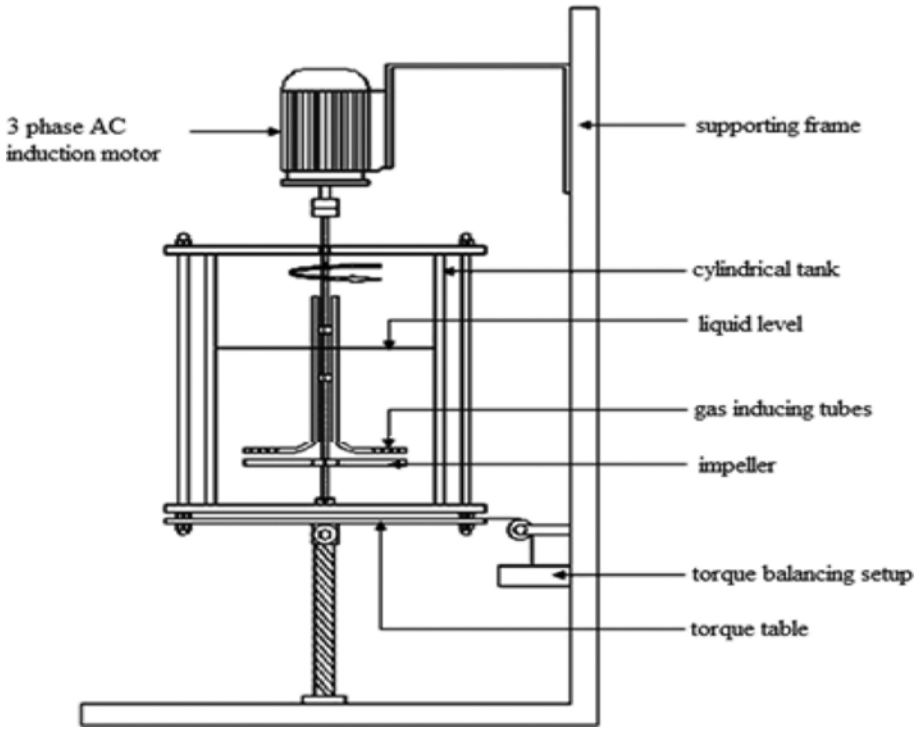

Fig. 1. Experimental setup of the conventional baffled agitated vessel retrofitted with the proposed air-inducing impeller system.

The tank was filled with water to the desired level and the motor was turned on. The speed of the impeller was gradually increased using speed-control-drive until the start of the suction of air, and the corresponding speed (critical speed) was measured with a tachometer. The initial liquid level and the increase in liquid level due to suction of air at higher rotational speeds of the impeller were noted down for computing the gas holdup. Critical speed for gas induction (N_c) is the minimum impeller speed at which the suction and distribution of the atmospheric air into liquid begins [17]. The critical speed was experimentally determined for air-inducing impeller system consisting of the air-inducing tube set and straight blade turbine impeller for gas-free liquid levels between 0.20 and 0.40 m with an increment of 0.05 m with a bottom clearance of 0.10 m. Critical Froude number (Fr_c) is the Froude number determined at critical impeller speed as

$$Fr_c = \frac{DN_c^2}{g} \tag{1}$$

where, D, N_c and g are impeller diameter, critical speed and acceleration due to gravity, respectively [17]. The gas-free liquid height, off-bottom clearance and the orifice submersion depth are combined into a single parameter called the dimensionless height determined by

$$h = \frac{H - C}{D_T} \tag{2}$$

where, H, C and D_T are the gas-free liquid level, off-bottom clearance of the impeller assembly and the diameter of the tank, respectively [17]. The power number (N_P) and the Reynolds number (N_{Re}) were determined as follows:

$$N_P = \frac{P}{\rho N^3 D^5} \tag{3}$$

$$N_{Re} = \frac{\rho N D^2}{\mu} \tag{4}$$

where, ρ and μ are the density and viscosity of the liquid, respectively.

For impeller speeds greater than the critical speed, the fractional gas holdup was determined by using the following equation:

$$\varepsilon_G = \frac{H_D - H}{H_D} \tag{5}$$

where, H is the height of the gas-free liquid and H_D is the height of dispersion [5].

RESULTS AND DISCUSSION

1. Critical Speed for Gas Induction

The critical Froude number (Fr_c), determined at various critical impeller speeds (N_c), was plotted against the dimensionless height (h) and the results are shown in Fig. 2. The critical Froude number increases with increase in dimensionless height [17]. It is because the critical speed for gas induction increases with increase in gas-free liquid level in the tank. From Eq. (2) it is clear that dimensionless height is directly proportional to the difference between the gas-free liquid level in the tank, and the off-bottom clearance tank diameter was not changed in this study. For a given gas-free liquid level, the orifice submergence depth decreases with increase in off-bottom clearance. Hence, the critical speed for gas induction increases with gas free liquid height and orifice submergence depth

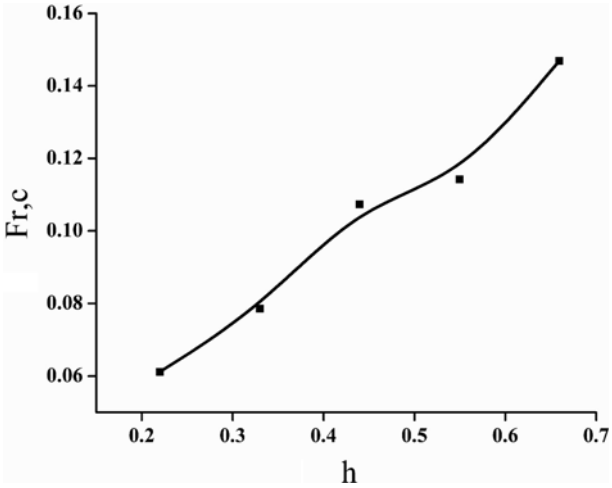

Fig. 2. Froude number at onset speed vs. dimensionless height for gas inducing tube set with straight blade turbine for a clearance of 0.1 m.

and decreases with the off-bottom clearance [5,18,19].

2. Power Consumption

2-1. Power Consumption at Different Reynolds Numbers

The effect of impeller speed on power consumption was studied by conducting experiments at impeller speeds in the range of 1.67-8.33 s^{-1} for gas-free liquid levels between 0.20 and 0.40 m with a increment of 0.05 m and a bottom clearance of 0.10 m. The power consumption was expressed in terms of Power number (N_P) using Eq. (3) and was plotted against the Reynolds number (N_{Re}) (see Fig. 3). As shown, the power number decreases with increase in Reynolds number and similar results were observed by some of the investigators [13,17]. The reason for decrease in power number with increase in Reynolds number is that the Reynolds number is directly proportional to the impeller speed, whereas the power number is inversely proportional to the third power (N^3) of the impeller speed and directly proportional to the power consumption.

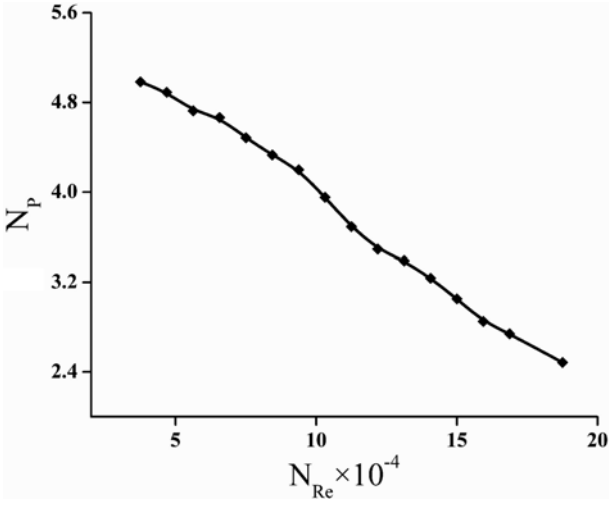

Fig. 3. Power number vs. Reynolds number for a liquid level of 0.2 m and a clearance of 0.1 m.

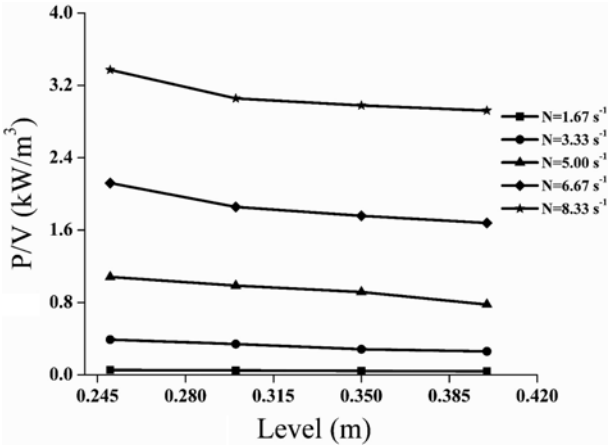

Fig. 4. Power consumption at different liquid levels and impeller speeds for gas inducing tube set with straight blade turbine for a clearance of 0.1 m.

2-2. Effects of Gas-free Liquid Height and Impeller Speed

The variation of power consumption with gas-free liquid height for various impeller speeds is shown in Fig. 4. It was observed that at lower impeller speeds, the power consumption is a weak function of the gas-free liquid height; however, at higher impeller speeds, the power consumption increases with increase in gas-free liquid height [7,12,17,20,21]. At lower impeller speeds, the power consumption depends mainly on the power required to displace the liquid at the impeller face, but at higher impeller speeds, the power consumption increases considerably due to many reasons, such as the impeller is subjected to a strong centrifugal force, the relative velocity between the impeller and the working fluid (liquid and gas bubbles in dispersion) etc. However, it was experimentally observed that at very high impeller speeds, the power consumption remains almost constant with increase in impeller speed as the density of the working fluid decreases when gas is induced at higher rate.

2-3. Effect of Impeller Assembly on Power Consumption

Power consumption per unit volume of the liquid was plotted

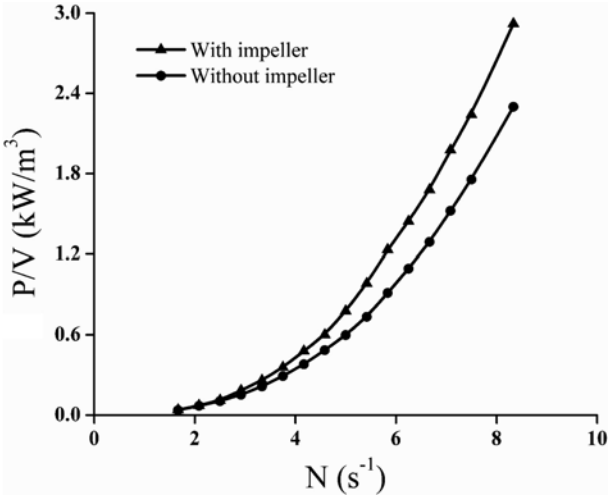

Fig. 5. Comparison of power consumption for gas-inducing tube set with and without straight blade turbine for a liquid level of 0.35 m and a clearance of 0.1 m.

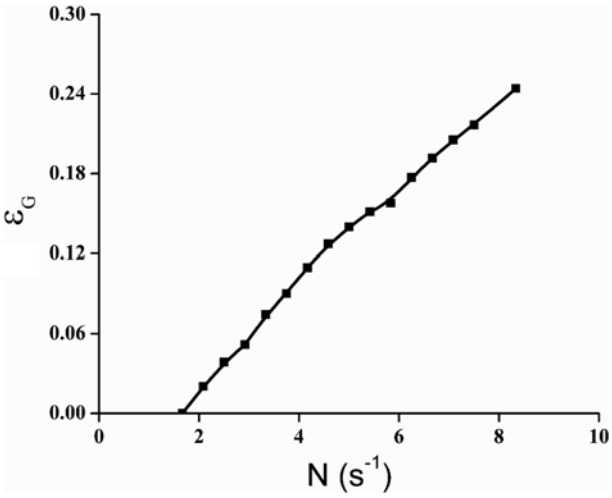

Fig. 6. Fractional gas holdup at different impeller speeds for gas inducing tube set with straight blade turbine for a liquid level of 0.2 m and a clearance of 0.1 m.

against the impeller speed for the gas-inducing tube set with and without the straight blade turbine impeller, and the results are shown in Fig. 5. The power consumption per unit volume increases with increase in impeller speed for both the cases [17,21]. Since the projected area, during rotation, of the impeller assembly increases when the impeller is attached to the impeller shaft, the power consumption for gas-inducing tube set with impeller is higher than that for gas-inducing tube set without impeller.

3. Fractional Gas Holdup

Fractional gas holdup is one of the vital parameters in the design of gas-inducing reactor systems. The variation in fractional gas holdup at different impeller speeds for gas-inducing tube set with straight blade turbine for a liquid level of 0.2 m and a clearance of 0.1 m and the results are depicted in Fig. 6. It is evident from the experimental results that the gas holdup continues to increase with increase in impeller speeds greater than the critical speed and becomes almost constant beyond a certain level of impeller speed [5, 15,19,22]. This is based on the fact that the gas holdup depends on the gas induction rate, which, in turn, is dependent on the impeller speed and the density of the working fluid. At the start of the gas induction, the density of the working fluid is relatively higher and hence the fractional gas holdup increases considerably with moderate increase in the impeller speed. However, at higher impeller speeds, the density of the working fluid continues to decrease with increase in gas induction. Since the gas induction rate and hence the fractional gas holdup are directly proportional to the impeller speed and the density of the working fluid, at higher impeller speeds, the presence of gas bubbles in the working fluid considerably decreases the density of the working fluid, which makes the gas induction rate as a weak function of impeller speed and results in no considerable further increase in both gas induction and hence the fractional gas holdup.

CONCLUSION

A novel method was developed for converting a conventional agitated vessel into a gas-inducing reactor with a retrofitted type of modification. A gas-inducing tube set was designed and fabricated which, when attached to the impeller shaft of a conventional agitated vessel, made it work like a gas-inducing reactor. The proposed experimental setup was tested for hydrodynamic studies. The critical speed for gas induction, power consumption per unit volume and gas holdup were determined and reported. The air-inducing impeller system used in this present study could induce the air at relatively lower impeller speeds. In fact, the experiments were conducted at impellers speeds up to 10 s^{-1} and the air could be induced under 3 s^{-1} in most of the operating conditions. This shows that this impeller system could induce the air at speeds lower than the critical speeds reported by most investigators. The method for air-induction demonstrated in this study eliminates the complications in the fabrication of air-inducing impeller system found in the literature and can be effectively used for converting all the existing agitated vessels readily into an air-inducing reactor by simple retrofitting type of modification.

NOMENCLATURE

C : impeller clearance from bottom of the tank [m]
D : diameter of the impeller [m]
D_T : diameter of the tank [m]
Fr : Froude number
Fr_c : Froude number at critical impeller speed
g : acceleration due to gravity [m s^{-2}]
H : total gas-free liquid height [m]
H_D : height of dispersion [m]
N : impeller speed [s^{-1}]
N_c : critical impeller speed [s^{-1}]
N_P : power number
N_{Re} : Reynolds number
P : power consumption [W]

Greek Letters

ε_G : fractional gas holdup (volumetric fraction of gas in the dispersion), dimensionless
μ : viscosity of liquid [kg m^{-1} s^{-1}]
ρ : density of liquid [kg m^{-3}]

REFERENCES

1. H. H. Vesselinov, B. Stephan, H. Uwe, K. Hogler, H. Gunther and S. Wilfried, *Chem. Eng. Res. Des.*, **86**, 75 (2008).
2. K. Saravanan, V. D. Mundale and J. B. Joshi, *Ind. Eng. Chem. Res.*, **33**, 2226 (1994).
3. K. Saravanan and J. B. Joshi, *Ind. Eng. Chem. Res.*, **34**(7), 2499 (1995).
4. A. W. Patwardhan and J. B. Joshi, *Ind. Eng. Chem. Res.*, **38**, 49 (1999).
5. F. Ju, Z.-M. Cheng, J.-H. Chen, X.-H. Chu, Z.-M. Zhou and P.-Q. Yuan, *Chem. Eng. Res. Des.*, **87**, 1069 (2009).
6. N. A. Deshmukh, S. S. Patil and J. B. Joshi, *Chem. Eng. Res. Des.*, **84**(A2), 124 (2006).
7. M. Jafari and J. S. S. Mohammadzadeh, *Chem. Eng. Res. Des.*, **83**(A5), 452 (2005).
8. A. D. Raidoo, K. S. M. S. Raghav Rao, S. B. Sawant and J. B. Joshi,

Chem. Eng. Commun., **54**, 1 (1987).
9. B. N. Murthy, R. B. Kasundra and J. B. Joshi, *Chem. Eng. J.*, **141**, 332 (2008).
10. S. E. Forrester, C. D. Rielly and K. J. Carpenter, *Chem. Eng. Sci.*, **53**(4), 603 (1998).
11. B. N. Murthy, N. A. Deshmukh, A. W. Patwardhan and J. B. Joshi, *Chem. Eng. Sci.*, **62**, 3839 (2007).
12. J.-H. Chen, Y.-C. Hsu, Y.-F. Chen and C.-C. Lin, *Water Res.*, **37**, 2919 (2003).
13. F. Scargiali, R. Russo, F. Grisafi and A. Brucato, *Chem. Eng. Sci.*, **62**, 1376 (2007).
14. S. H. Lin and C. H. Wang, *J. Hazard. Mater.*, **B98**, 295 (2003).
15. J.-J. Zhong, *Korean J. Chem. Eng.*, **27**(4), 1035 (2010).
16. A. Saptoro, M. T. H. Herng and E. L. W. Teng, *Korean J. Chem. Eng.*, **31**(4), 650 (2014).
17. M. Jafari and J. S. S. Mohammadzadeh, *Chem. Eng. J.*, **103**, 1 (2004).
18. C. D. Rielly, G. M. Evans, J. F. Davidson and K. J. Carpenter, *Chem. Eng. Sci.*, **47**(13-14), 3395 (1992).
19. S. Poncin, C. Nguyen, N. Midoux and J. Breysse, *Chem. Eng. Sci.*, **57**, 3299 (2002).
20. Y.-C. Hsu, R. Y. Peng and C. Jih, *Chem. Eng. Sci.*, **52**(21, 22), 3883 (1997).
21. R. Fakuda, M. Tokumura, H. T. Z. and Y. Kawase, *Chem. Eng. Res. Des.*, **87**, 452 (2009).
22. N. A. Deshmukh and J. B. Joshi, *Chem. Eng. Res. Des.*, **84**(A11), 977 (2006).